



## Factors influencing the operational stability of NADPH-dependent alcohol dehydrogenase and an NADH-dependent variant thereof in gas/solid reactors

Liliya Kulishova<sup>a,1</sup>, Kerasina Dimoula<sup>b,1</sup>, Max Jordan<sup>b</sup>, Astrid Wirtz<sup>a</sup>, Diana Hofmann<sup>c</sup>, Beatrix Santiago-Schübel<sup>c</sup>, Jörg Fitter<sup>d</sup>, Martina Pohl<sup>a,\*</sup>, Antje C. Spiess<sup>b,\*\*</sup>

<sup>a</sup> Institute of Molecular Enzyme Technology, University of Düsseldorf, D-52426 Jülich, Germany

<sup>b</sup> AVT-Biochemical Engineering, RWTH Aachen University, Worringerweg 1, D-52074 Aachen, Germany

<sup>c</sup> ZCH/BioSpec, Forschungszentrum Jülich GmbH, D-52425 Jülich, Germany

<sup>d</sup> Institute of Structural Biology and Biophysics 2, Forschungszentrum Jülich GmbH, D-52425 Jülich, Germany

### ARTICLE INFO

#### Article history:

Received 25 March 2010

Received in revised form 20 July 2010

Accepted 14 September 2010

Available online 22 September 2010

#### Keywords:

Operational stability

Thermostability

Gas/solid bioreactor

NAD(P)H

Alcohol dehydrogenase

### ABSTRACT

The continuous enzymatic gas/solid bio-reactor serves both for the production of volatile fine chemicals and flavors on an industrial scale and for thermodynamically controlled investigation of substrate and water effects on enzyme preparations for research purposes. Here, we comparatively investigated the molecular effects on the operational stability of NADPH-dependent *Lactobacillus brevis* alcohol dehydrogenase and an NADH-dependent variant thereof, LbADH G37D, in the gas/solid bioreactor. The reference reaction is the reduction of acetophenone to (*R*)-1-phenylethanol with concomitant oxidation of 2-propanol to acetone for the purpose of regeneration of the redox cofactor.

It could be clearly shown that not the thermostability of the cofactor, but the thermostability of the proteins in the solid dry state govern the order of magnitude of the operational stability of both purified enzymes in the gas/solid reactor at low thermodynamic activity of water and substrate. However, at higher thermodynamic activity the operational stability in the gas/solid reactor is overlaid by stabilizing and destabilizing effects of the substrates that require further investigation. We demonstrated first evidence that the substrate affinity of the two variants in the gas/solid reactor is similar to the affinity in aqueous medium. We could also show that partial unfolding of the proteins with subsequent aggregation are the factors governing protein thermo-in-stability both in the dissolved and in the dry state. Thus, stability investigations of enzymes in the dry state are suggested to predict their basal level of operational stability in gas/solid reactions.

© 2010 Elsevier B.V. All rights reserved.

### 1. Introduction

Gas/solid biocatalysis represents an alternative to common liquid biocatalytic reaction systems, where the solid dry enzyme catalyzes conversion of gaseous substrates to gaseous products. The technology is used for production of volatile compounds like esters and alcohols [1]. It exhibits significant advantages, such as high pro-

ductivity, pronounced stability of the immobilized biocatalyst [2] and simplified downstream processing [3]. The possibility to control thermodynamic parameters in a gas/solid system additionally allows adjusting the enzyme micro-environment, which is important for scientific purposes, such as studies of enzyme hydration or solvent influences [4].

It is generally accepted that dry enzymes are significantly more stable than the dissolved ones. However, progressive inactivation of alcohol dehydrogenases is observed under the gas/solid reactor conditions [5–8]. Yang and Russell described the conversion of 3-methyl-2-buten-1-ol, catalyzed by immobilized yeast alcohol dehydrogenase in a continuous gas/solid reactor at 22–50 °C at different water activities and observed steady-state periods of 4–16 days prior to progressive inactivation [8]. Reduction of acetophenone with the solid immobilized wild type ADH from *Lactobacillus brevis* (LbADHwt) performed in a continuous gas/solid reactor at 40 °C and a water activity ( $a_w$ ) of 0.5 revealed a half-life between 1 and more than 40 days for the enzymatic activity depending on the immobilization conditions [7]. Up to now the mecha-

**Abbreviations:** AcPh, acetophenone;  $a_w$ , water activity; BSA, bovine serum albumin; HPLC/MS, high pressure liquid chromatography/mass spectroscopy; LbADH, *Lactobacillus brevis* alcohol dehydrogenase; RT, room temperature; TEA, triethanolamine; wt, wild type.

\* Corresponding author. Present address: Institute of Biotechnology 2, Forschungszentrum Jülich GmbH, D-52425 Jülich, Germany. Tel.: +49 0246 1614388.

\*\* Corresponding author. Tel.: +49 241 8028111; fax: +49 241 8022570.

E-mail addresses: [ma.pohl@fz-juelich.de](mailto:ma.pohl@fz-juelich.de) (M. Pohl), [antje.spieess@avt.rwth-aachen.de](mailto:antje.spieess@avt.rwth-aachen.de) (A.C. Spiess).

<sup>1</sup> Both authors contributed equally to this work.

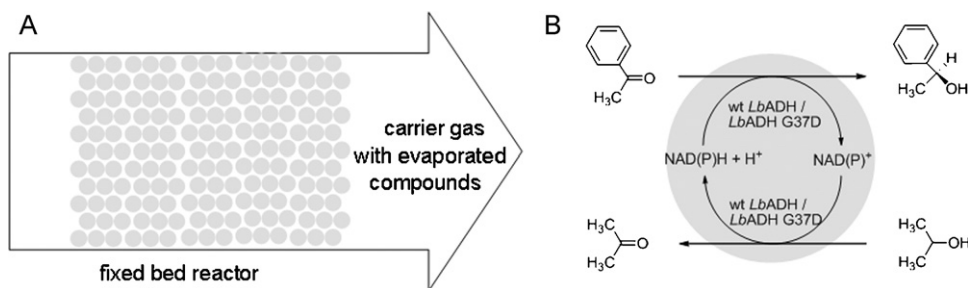


**Fig. 1.** Biocatalytic reduction of acetophenone in a gas solid reactor. (A) Reaction principle of passing gas mixture across a fixed bed of immobilized enzyme preparation. (B) The cofactor NAD(P)H is regenerated by a substrate coupled approach using 2-propanol as a second substrate.

nisms leading to enzyme inactivation in the solid state remain unclear.

To elucidate the effects of temperature on activity and stability, previous studies focused on the comparison of operational stabilities of ADHs derived from different thermophilic and mesophilic sources [9]. It was shown that high thermal stability in aqueous media was not necessarily correlated with higher stability under gas/solid reactor conditions [9]. However, the enzymes used in that study were from different organisms, showing significant sequence and structural differences. Engineered enzymes, differing only in few sequence positions were never comparatively studied in the gas/solid system.

Here we present a comparative study of the NADPH-dependent wild type ADH from *L. brevis* (*LbADH*<sub>w</sub>) and the NADH-dependent variant thereof, *LbADH* G37D. Both are able to reduce ketones to the corresponding (*R*)-alcohols with high stereoselectivity [10,11]. As can be deduced from structural data, both enzyme variants are homotetramers with a molecular weight of 107 kDa, they contain two Mg<sup>2+</sup> binding sites and four active centres (one per subunit) [11,12]. The variant was created to accept cheaper and more stable cofactor NADH [13,14] with higher affinity than NADPH [11].

Activity and stability of the *LbADH*<sub>w</sub> and the *LbADH* G37D were studied in aqueous solution, in the dry solid state and with respect to their operational stability in a gas/solid reactor (see principle in Fig. 1A). To identify the main factors causing enzyme inactivation in the gas/solid system, the reduction of acetophenone to (*R*)-1-phenylethanol with concomitant oxidation of 2-propanol to acetone for the cofactor regeneration was studied (Fig. 1B), while varying thermodynamic parameters, such as water activity, and acetophenone activity. Additionally, the thermostability of both enzyme variants and the cofactors was investigated in the solid state and in solution using tryptophan fluorescence spectroscopy and HPLC/MS, respectively.

## 2. Results and discussion

In case of substrate-coupled cofactor regeneration the cofactors for the biocatalytic reduction step are required in equimolar amounts with respect to the enzyme's active sites, here four per *LbADH* molecule. Therefore, the cofactor stability in the gas/solid reactor is as important as the stability of the respective enzyme. In aqueous solution the oxidized and the reduced cofactor molecules are able to freely diffuse between the binding site in the enzyme and the solution, enabling substrate coupled and enzyme coupled cofactor regeneration [15]. The situation is different in gas/solid biocatalysis, as the cofactor remains in the enzyme's active site and must be regenerated by a substrate coupled approach. As a consequence, inactivated cofactor molecules remain in the active sites and render the respective site inactive. There are currently no data available concerning the stability of NAD(P)H in the dry state. Thus, our studies started with a detailed investigation of the stability of the reduced cofactors in the liquid and dry state.

### 2.1. Thermostability of NAD(P)H

Up to now, the stability of the redox cofactors has exclusively been studied in aqueous solution, demonstrating that NADH is significantly more stable than NADPH under various conditions, such as alkaline or acidic pH or elevated temperature [13,16–19]. Additionally, these studies showed that factors such as buffer salt, ionic strength, and pH increase the speed of NAD(P)H degradation even at moderate temperatures [13,18,19]. In order to obtain the respective data for the solid phase, we studied the thermal stability of NAD(P)H under the same conditions (buffer, ionic strength and pH) as used for the immobilization of the enzyme and compared their stability in the solid and the dissolved state.

The thermal stability of the dissolved cofactor at pH 7.2 was analyzed in a temperature range of 30–70 °C by measuring the decay of absorbance at 340 nm, which is proportional to the concentration of reduced nicotinamide moieties. Further, the residual reducing activity of the heat-treated cofactor samples was studied by the standard activity assay using the *LbADH*<sub>w</sub> for NADPH and the variant *LbADH* G37D for NADH (Fig. 2). In separate experiments the thermal degradation products derived after thermal treatment of the solid cofactor probes for 16 h at 95 °C were analyzed by HPLC/MS analysis (see below).

The absorption at 340 nm and the residual activity decreased over time following a linear decay at lower temperatures and a single-order exponential decay at higher temperatures (Fig. S1, supplementary material). The estimated half-life significantly decreased with increasing temperature for both NADH and NADPH. As expected, the dissolved NADH was 3.5–5.5 times more thermostable than the phosphorylated cofactor. In a range of 30–60 °C, half-life values calculated from residual activity measurements were 20–50% lower than the ones estimated from absorbance<sub>340</sub> decay curves. The tendency was more pronounced for NADPH. This fact indirectly suggests the presence of enzymatically inactive degradation products containing a reduced nicotinamide ring. At 70 °C half-life values measured by both methods were statistically the same. Thermal stabilities of the solid cofactor samples were examined by the same techniques, absorbance<sub>340</sub> and reducing activity (Fig. 3).

Surprisingly, the solid cofactors were stable for several weeks upon incubation at 50 °C, as was indicated by a constant absorbance at 340 nm (Fig. 3A). However, the corresponding reducing activity of NADPH gradually decreased to approximately 60% of the initial activity (Fig. 3B), whereas both the absorbance<sub>340</sub> and the reducing activity of the solid NADH remained almost unchanged (Fig. 3). In comparison to the half-life of > 24 days at 50 °C for both solid cofactors, half-life of dissolved NADPH and NADH at 50 °C equaled to 60 ± 1 and 240 ± 20 min, respectively.

Due to the slow degradation process, the incubation temperature of the solid samples was increased to 95 °C to study the degradation products after 16 h by HPLC/MS. Interestingly, even under these harsher conditions, a significant part of the solid

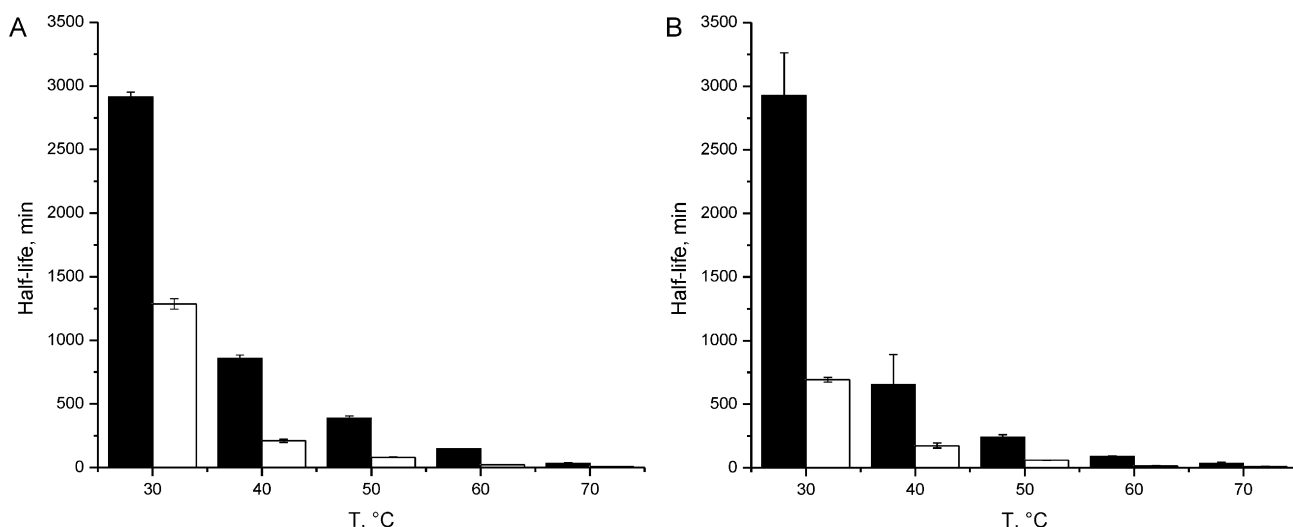


**Fig. 2.** Thermal stability of dissolved NADH (black) and NADPH (white). Half-life was determined by (A) following the decay of absorbance at 340 nm by measuring the residual reducing activity in the standard activity assay and by (B) measuring the residual reducing activity in the standard activity assay by following the decay of absorbance at 340 nm. Initial cofactor concentration was 9.5 mM in 50 mM TEA, pH 7.2, for the activity assay it was diluted to 0.19 mM. Fig. S1 shows detailed results for all temperatures studied.

cofactor samples remains intact. The same is true for the dissolved cofactor samples that have been incubated at 50 °C for 16 h. (Table 1).

From the data in Table 1 it is clearly visible that the thermal degradation of NADH and NADPH occurs in different ways. More degradation products were detected after heat treatment of solid NADPH than of solid NADH. Whereas in case of NADH almost all observed fragments occur in both the liquid and the solid sample, differences concerning the fragmentation pattern were observed with NADPH, where fragments 2a, 3a, 6a, 9a and 10a were only observed in the solid state. Main fragmentation routes include the cleavage of the nicotin amide ring as well as oxidative ring opening of the ribose rings. Further, cleavage of the phosphoester bonds is observed yielding adenosine mono-, di- and tri-phosphate. According to the different retention times observed in HPLC the AMP (9a and 8b) and ADP fragments (8a and 7b) can be regarded as different concerning the position of the phosphate groups (Table 1). Both cofactors show enzymatically inactive degradation products containing an intact reduced nicotinamide ring (3a, 4a, 3b, 5b) (Table 1) giving rise to absorbance at 340 nm, which explains the differences observed in half-life determination based on residual

activity determinations and absorbance measurements at 340 nm (see above).

To conclude, although the stability of redox cofactors in the solid state is significantly higher than in aqueous solution, the higher stability of NADH compared to NADPH has been proven also in the solid state. Therefore, the use of NADH-dependent oxidoreductases in gas/solid systems might be one possibility to increase the stability of such systems.

## 2.2. Preparation and basic characterization of variants in gas/solid reactor

The preparation, purification and kinetic as well as structural characterization of a NADH-dependent variant of the *L. brevis* alcohol dehydrogenase by a single amino acid exchange, *LbADH* G37D, was reported earlier [11]. In solution at pH 7 the NADH-dependent variant *LbADH* G37D has a roughly 12 times lower enzymatic activity (7 U/mg) compared to the NADPH-dependent *LbADH*wt (90 U/mg). Thus, a higher amount of biocatalyst in the gas/solid reactor was considered essential for the variant in order to compensate its expected lower activity and obtain measurable reaction

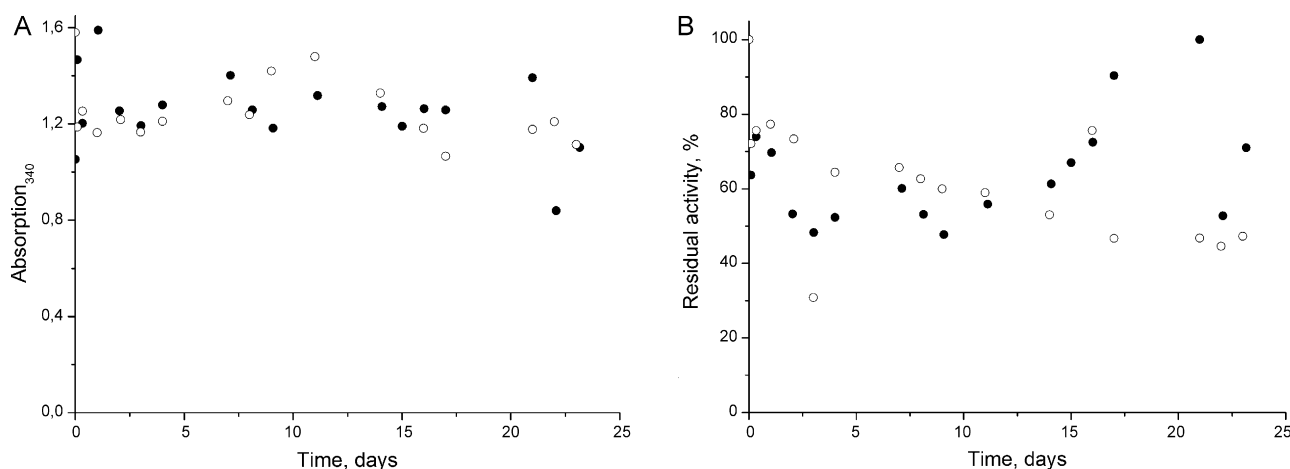


**Fig. 3.** Thermal stability of solid NADH (black) and NADPH (white) at 50 °C by analysis of absorbance<sub>340</sub> (A) and relative activity (B). Solid cofactor samples were incubated at 50 °C for a time intervals of 0–23 days, dissolved in 50 mM TEA buffer, pH 7.2 and analyzed for the absorbance at 340 nm and the residual reducing activity in the standard activity assay. Initial cofactor concentration after redilution was 9.5 mM in 50 mM TEA, pH 7.2, for the tests it was further diluted to 0.19 mM.

**Table 1**  
Comparison of NADH and NADPH thermal degradation products (neutral masses) after 16 h in solid state at 95 °C and in water at 50 °C obtained by HPLC/MS. Occurrence of the compound or degradation product for the particular sample is indicated by x. -: fragment not found.

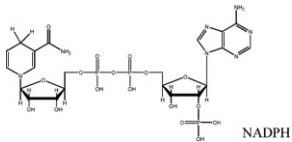
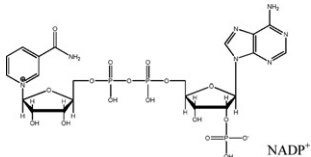
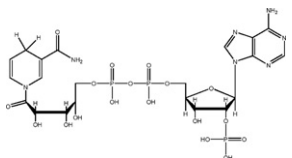
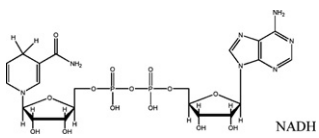
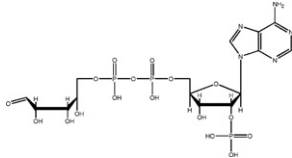
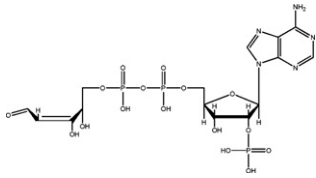
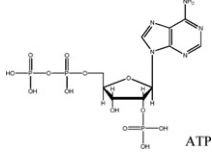
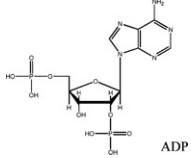
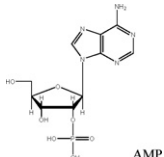
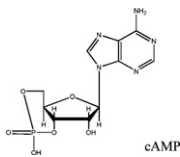
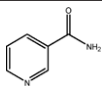
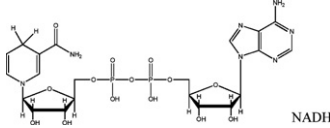
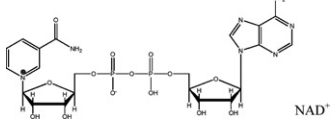
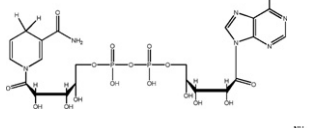
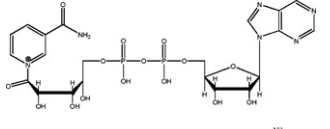
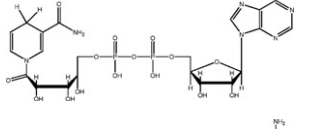
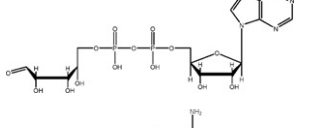
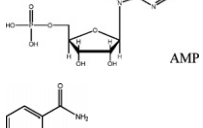
Peak number	Degradation products of NADPH				
	Mass (Da)	Structure	NADPH solid	NADPH dissolved	Retention time (min)
1a	745	 NADPH	x	x	14.5
2a	743	 NADP <sup>+</sup>	x	-	16.0
3a	761	 NADPH	x	-	24.3
4a	665	 NADH	x	x	6.5
5a	639	 NADH	x	x	22.3
6a	621	 NADH	x	-	15.7
7a	507	 ATP	x	x	15.8
8a	427	 ADP	x	x	14.0
9a	347	 AMP	x	-	6.0
10a	329	 cAMP	x	-	10.0

Table 1 (Continued)

Peak number	Degradation products of NADPH				
	Mass (Da)	Structure	NADPH solid	NADPH dissolved	Retention time (min)
11a	122		x	x	3.9
Degradation products of NADH					
1b	665		x	x	6.5
2b	663		x	x	7.8
3b	697		x	–	12.3
4b	679		x	x	8.0
5b	681		x	x	9.3
6b	559		x	x	8.5
7b	427		x	x	7.9
8b	347		x	x	8.5
9b	122		x	x	3.9

rates. A direct comparison of the two variants in the gas/solid reactor, however, requires the same amount of deposited lyophilized protein per gram of carrier for both enzymes. This is essential to avoid potential differences in the micro-environment of the two enzyme preparations such as different levels of adsorption of water and substrates that could result in different activity and stability in the gas/solid reactor [20]. A variation of the amount of carrier in the gas/solid reactor with constant 2.8 mg/g lyophilized protein loading did not influence the enzyme stability as expected and shown for *LbADH* G37D (see Fig. S2, supplementary material). The half-life of *LbADH* G37D remained almost constant at the average of 22 h, when increasing the amount of loaded carrier from 50 to 400 mg. The progress curves of the reaction, for all catalyst loadings, were almost

identical. As the loading of the reactor obviously does not influence the stability of the deposited enzyme, the remaining parameters, namely thermodynamic activity of water and acetophenone, were studied with 50 mg carriers for wild type *LbADH* and 100 mg carriers for *LbADH* G37D, resulting in doubled total protein amount in the reactor for the variant *LbADH* G37D.

### 2.3. Effect of water activity on operational stability and activity of *LbADH* variants

In contrast to enzymatic reactions performed in solution, it is possible to individually adjust the thermodynamic activity of any compound to the desired level in the gas/solid system. Thus

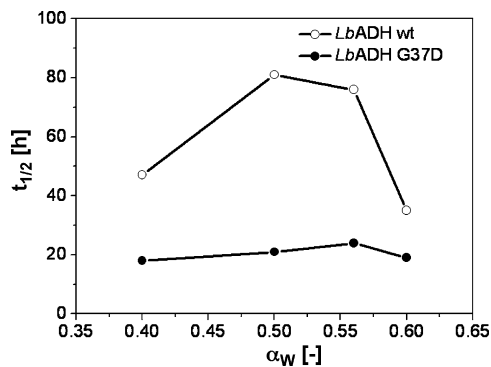


**Fig. 4.** Effect of water activity on the operational enzyme stability in the gas/solid reactor. Half-life was obtained from the conversion obtained in continuous fixed bed reactor experiments under the following operating conditions:  $\alpha_{\text{AcPh}} = 0.3$ ,  $n_{2\text{-prop}}/n_{\text{AcPh}} = 60$ ,  $m = 50$  mg (LbADHwt),  $m = 100$  mg (LbADH G37D),  $V_{\text{tot}} = 20$  mL/min,  $T = 40^\circ\text{C}$ .

the influence of the ‘key parameter’ water activity ( $a_w$ ) [4] on the activity and stability of the enzyme was studied, keeping all other reaction conditions unaffected. First, the water activity of the gaseous reaction mixture was varied between  $a_w$  0.4 and 0.6 and its influence on the stability of LbADHwt and LbADH G37D was monitored (Fig. 4).

Unexpectedly, NADPH-dependent LbADHwt appeared to be more stable in the gas/solid system than the NADH-dependent LbADH G37D. The half-life of LbADHwt varied between 30 and 80 h, and amounted to 2–4-fold the half-life of LbADH G37D (Fig. 4). With regard to the high stability of both cofactors in the dry state (rf. to Fig. 3), this fact indicates that the cofactor stability is probably not the decisive parameter for the enzyme stability in the gas/solid reaction system. As demonstrated in Fig. 4, the stability of the purified wild type enzyme shows a maximum at  $a_w = 0.5$ . This result contradicts to the previous findings with crude cell extract preparations of LbADHwt [2] that indicated a continuously decreasing stability of the deposited enzyme in the gas/solid reactor with increasing water activity. The observed maximum, however, is in line with studies on purified thiamine diphosphate-dependent enzymes that also revealed an optimal stability at a water activity of 0.5 [21]. In contrast, the stability of deposited lyophilized LbADH G37D was almost independent of the water activity within the range studied (Fig. 4).

In the same experiments, the initial specific reaction rate achieved by the two enzyme variants was evaluated at different water activities and – in contrast to the stability behaviour – showed the expected trends. The initial specific reaction rate was expressed in  $\mu\text{mol}/\text{min}/\text{mg}$  relative to the total protein amount in the reactor (Fig. 5).

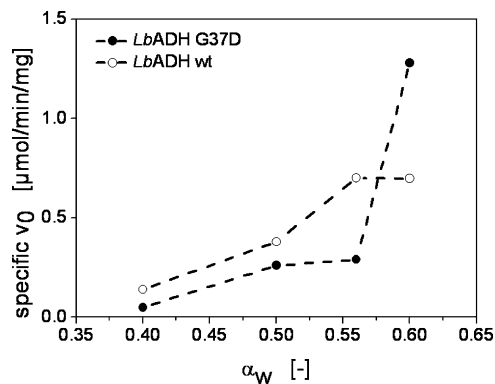


**Fig. 5.** Effect of water activity on specific initial reaction rate in the gas/solid reactor.  $\alpha_{\text{AcPh}} = 0.3$ ,  $n_{2\text{-prop}}/n_{\text{AcPh}} = 60$ ,  $m = 50$  mg (LbADHwt),  $m = 100$  mg (LbADH G37D),  $V_{\text{tot}} = 20$  mL/min,  $T = 40^\circ\text{C}$ .

With increasing water activity, the expected increase of the initial specific reaction rate of the two enzyme variants was observed (Fig. 5). Whereas the specific initial reaction rate of LbADH G37D increased continuously with increasing water activity, the initial reaction rate of the wild type enzyme did not increase beyond  $a_w = 0.55$ . This could imply a faster thermal denaturation of the wild type enzyme that overlaps the increased flexibility and thereby increased activity of the enzyme at higher water activities. The specific initial reaction rates of both enzyme variants in the gas/solid reactor were found to be of the same order of magnitude, in contrast to the enzyme activities in solution where LbADHwt was found to be 12 times faster than LbADH G37D. Thus, the performance of the G37D variant in the gas/solid system was found to be improved compared to its performance in solution.

#### 2.4. Effect of acetophenone activity on the operational stability and activity of variants

Besides the influence of the water activity, the gas/solid reactor does also allow investigating the enzyme variants as a function of the thermodynamic activity of the substrates. For this study, the water activity was fixed at 0.5, for which maximal stability of the wild type enzyme was observed. The acetophenone activity was then varied in the range of 0.14–0.3, simultaneously varying the 2-propanol activity and thus keeping the molar ratio of the two substrates constant (Fig. 6).

LbADH G37D has approximately the same operational stability as the wild type enzyme, with the highest difference in half-life of 60 h at the highest acetophenone activity investigated. Differences in half-life between the variants at lower substrate activities

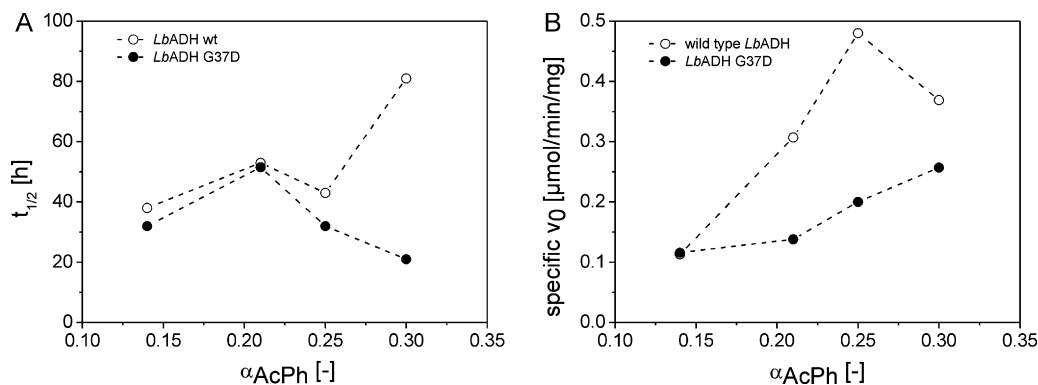


**Fig. 6.** Effect of substrate activity in the gas/solid reactor on (A) stability and (B) initial specific reaction rate relative to deposited protein amount:  $a_w = 0.5$ ,  $\alpha_{\text{AcPh}} = 0.3$ ,  $n_{2\text{-prop}}/n_{\text{AcPh}} = 60$ ,  $m = 50$  mg (wild type LbADH),  $m = 100$  mg (LbADH G37D),  $V_{\text{tot}} = 20$  mL/min,  $T = 40^\circ\text{C}$ .

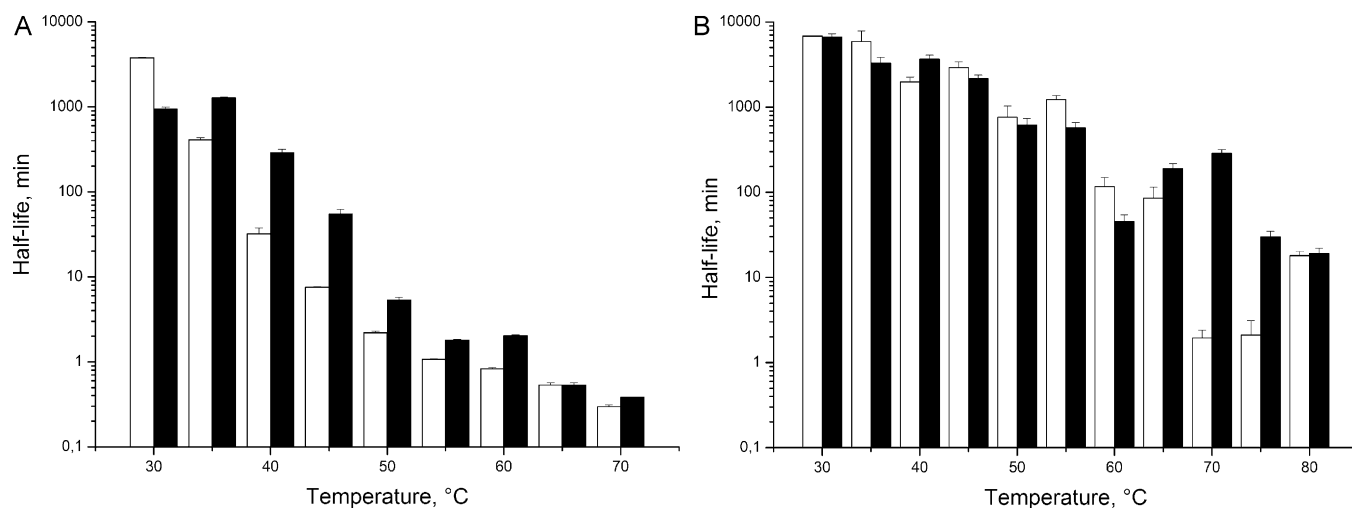


**Fig. 7.** Thermal stability of *LbADHwt* (white) and *LbADH G37D* (black) in the dissolved (A) and the solid state (B). Heat inactivation experiments were performed with 100  $\mu$ L of the 0.1 mg/mL enzyme solution in 10 mM TEA, 1 mM  $MgCl_2$ , pH 7.2 (A) or with the solid sample obtained after freeze-drying of 100  $\mu$ L of 0.1 mg/mL enzyme in 10 mM TEA, 1 mM  $MgCl_2$ , pH 7.2 (B). The enzymatic activity was measured at 30 °C; the assay mixture contained 11 mM acetophenone, 0.19 mM NAD(P)H, 1 mM  $MgCl_2$  in 50 mM TEA buffer.

ranged within the experimental error of 1–5 h. The variant *LbADH G37D* showed a maximal stability at an intermediate  $a_{AcPh}$  of 0.21, nearly matching the half-life of *LbADHwt* under these conditions (52 h). In contrast, *LbADHwt* exhibited an increasing stability with increasing substrate activity (Fig. 6A). Theoretically, the observed differences in operational stability should be due to one of the following reasons:

- The single amino acid exchange might change the general protein stability in the dry state and will therefore be investigated below as a separate phenomenon.
- A single amino acid exchange might also change the protein microenvironment by changing the protein surface amino acids and thus the affinity of polar and non-polar compounds to the protein, leading to changed protein stability in the presence of substrates. However, in the present case, the amino acid was exchanged in the active site and is not exposed to the protein surface.
- The single amino acid exchange in the active site does also impact the catalytic properties of the enzyme, such as substrate affinity or substrate inhibition, thus generating effects overlaying with the higher protein stability in the presence of the substrates. Some changed catalytic behaviour of the variant *LbADH G37D* has been shown in solution [11] and is now discussed for the gas/solid reactor (Fig. 6B).

The initial specific reaction rates with respect to the deposited protein amount were also evaluated as a function of the acetophenone activity and – similar to the effect of water activity – were found to be of the same order of magnitude (Fig. 6B). The number of data points of this investigation is not sufficient to allow for quantitative evaluation of kinetic parameters for the two enzyme variants in the gas/solid reactor. But obviously, within the tested substrate activity range, no saturation for the variant *LbADH G37D* is observed, but a nearly linear increase of the initial specific reaction rate with substrate activity. In contrast, *LbADHwt* seems to have reached a plateau above a substrate activity of 0.20 (Fig. 6B). This corresponds to the effects of the amino acid exchange observed before in solution experiments, where the variant *LbADH G37D* exhibits higher  $K_m$  values both for its cofactor and both substrates, increasing the saturation level in solution significantly [11] (see Table S1, supplementary material). In solution,  $K_m$  values for acetophenone equaled to 2.8 mM and 10.9 mM for the *LbADHwt* and

*LbADH G37D*, respectively [11], whereas the cofactors'  $K_m$  values amounted to 0.04 mM (NADPH) for *LbADH wt*, and 1.6 mM (NADH) for *LbADH G37D*. Obviously, the single amino acid exchange G37D has indeed a significant impact on catalysis. Thus, in order to fully understand the operational stability of the two variants, the influence of the substrate activity both under reactive and non-reactive conditions should be further investigated in future, at different water activity levels and probably also at varying relative and/or absolute 2-propanol and acetophenone activity levels.

### 2.5. Influence of the dry and liquid state on the thermostability of variants

The operational studies in the gas/solid reactor gave several indications that the catalytic properties of the enzyme variants in the non-conventional solid state are very different compared to studies in solution. To exclude the catalytic effects on the stability, both enzyme variants were comparatively studied in solution and in the solid state without the presence of the substrates acetophenone and 2-propanol, thus restricting the measurements to the thermostability of the enzyme variants. Thermal stabilities of *LbADHwt* and the variant were expressed as half-life of the residual activity after incubation at elevated temperatures (Fig. 7). The samples of the dissolved enzymes were subjected to analysis directly after heating, whereas the solid samples were cooled down on ice and re-dissolved in water prior to the measurement.

Fig. 7A shows the half-life of the dissolved *LbADHwt* in the range of 30–80 °C compared to the variant under the same conditions. For both dissolved enzyme variants, half-life non-linearly decays with increasing temperature. In the temperature range of 35–60 °C the NADPH-dependent wild type enzyme shows a 2–9-fold lower thermal stability in the dissolved state than the NADH-dependent variant G37D. Data points at 30 °C and 70 °C are hard to compare, because the slow inactivation at 30 °C and the fast inactivation at 65 °C and 70 °C made half-life calculation inaccurate. Both enzyme variants are approximately two orders of magnitude more stable in the solid state than in solution (Fig. 7). In solution, the cofactor becomes more stable than the protein already above temperatures between 32.5 and 34.5 °C for the pairs of NADPH/wt*LbADH* and NADH/*LbADH G37D*, respectively. In the solid state, the cofactor is more stable than the protein for all temperatures investigated.

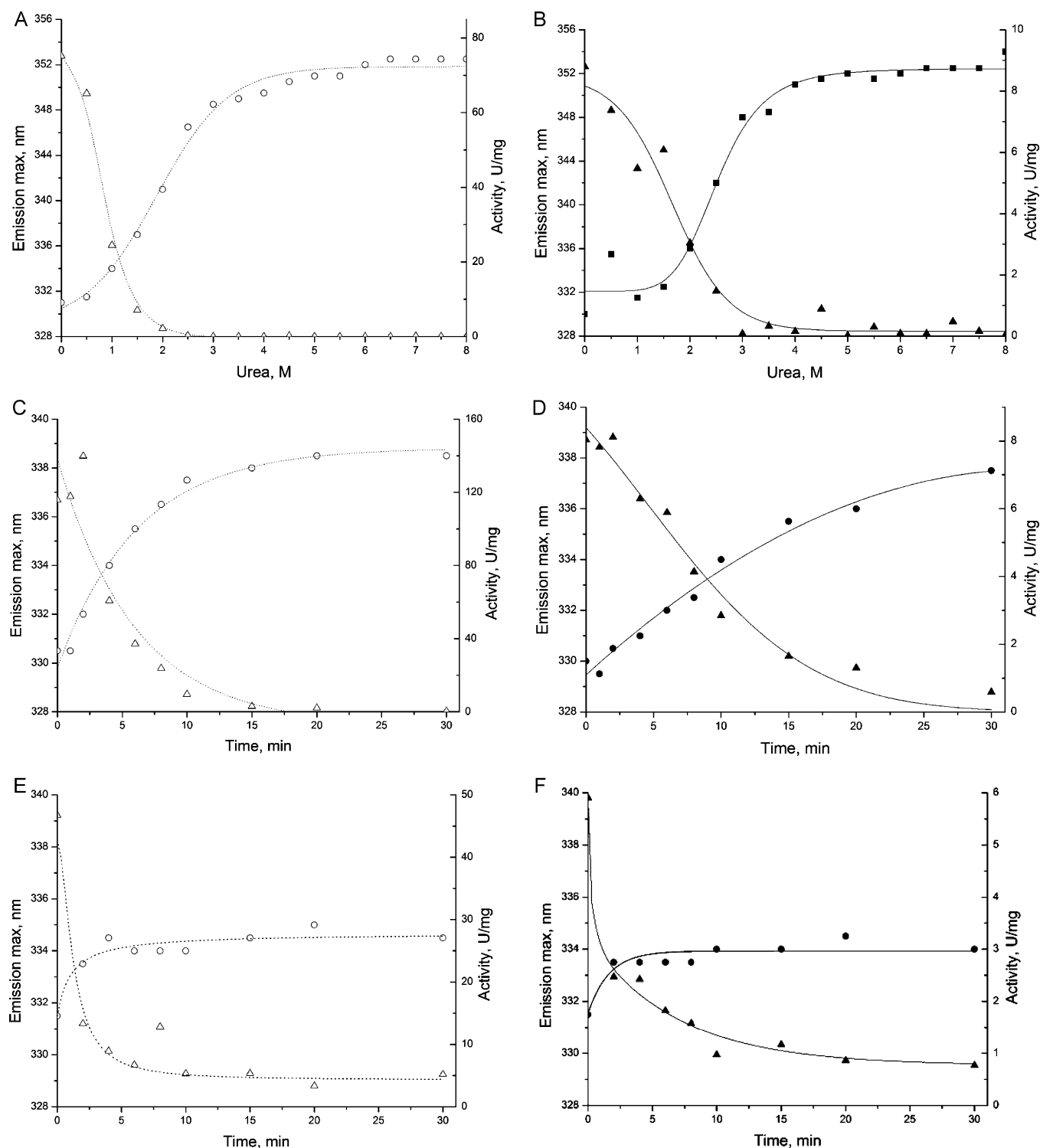


**Fig. 8.** Thermal inactivation and unfolding of *LbADHwt* (white) and *LbADH G37D* (black). Tryptophane fluorescence emission maxima are depicted in circles, residual activity data (calculated based on total protein amount) are represented by triangles. A: *LbADHwt* denaturation in the presence of urea; B: *LbADH G37D* denaturation in the presence of urea; C: dissolved *LbADHwt* at 50°C; D: dissolved *LbADH G37D* at 50°C; E: solid *LbADHwt* at  $a_w = 0.1$  and  $T = 80^\circ\text{C}$ ; F: solid *LbADH G37D* at  $a_w = 0.1$  and  $T = 80^\circ\text{C}$ . For fluorescence spectroscopy samples were excited at 295 nm (slit: 7.5 nm) in a 1 cm cuvette and emission spectra were recorded in the range of 300–450 nm (slit: 7.5 nm) at 25°C.

At 40°C, at the temperature of the operational stability investigations (Figs. 4 and 6A), the protein half-life in the solid state without substrates present amounted to 33 and 58 h for *LbADHwt* and *LbADH G37D*, respectively. These values for protein thermostability are in the same order of magnitude as those for the operational stability in the presence of defined thermody-

namic activities of water and substrates with operational half-life between 20 and 80 h. As mentioned earlier, the observed differences in half-life under operational conditions between the two variants are significantly reduced at lower acetophenone activity (Fig. 6A). Thus, protein thermostability seems to be the major influence factor determining operational stability in the gas/solid

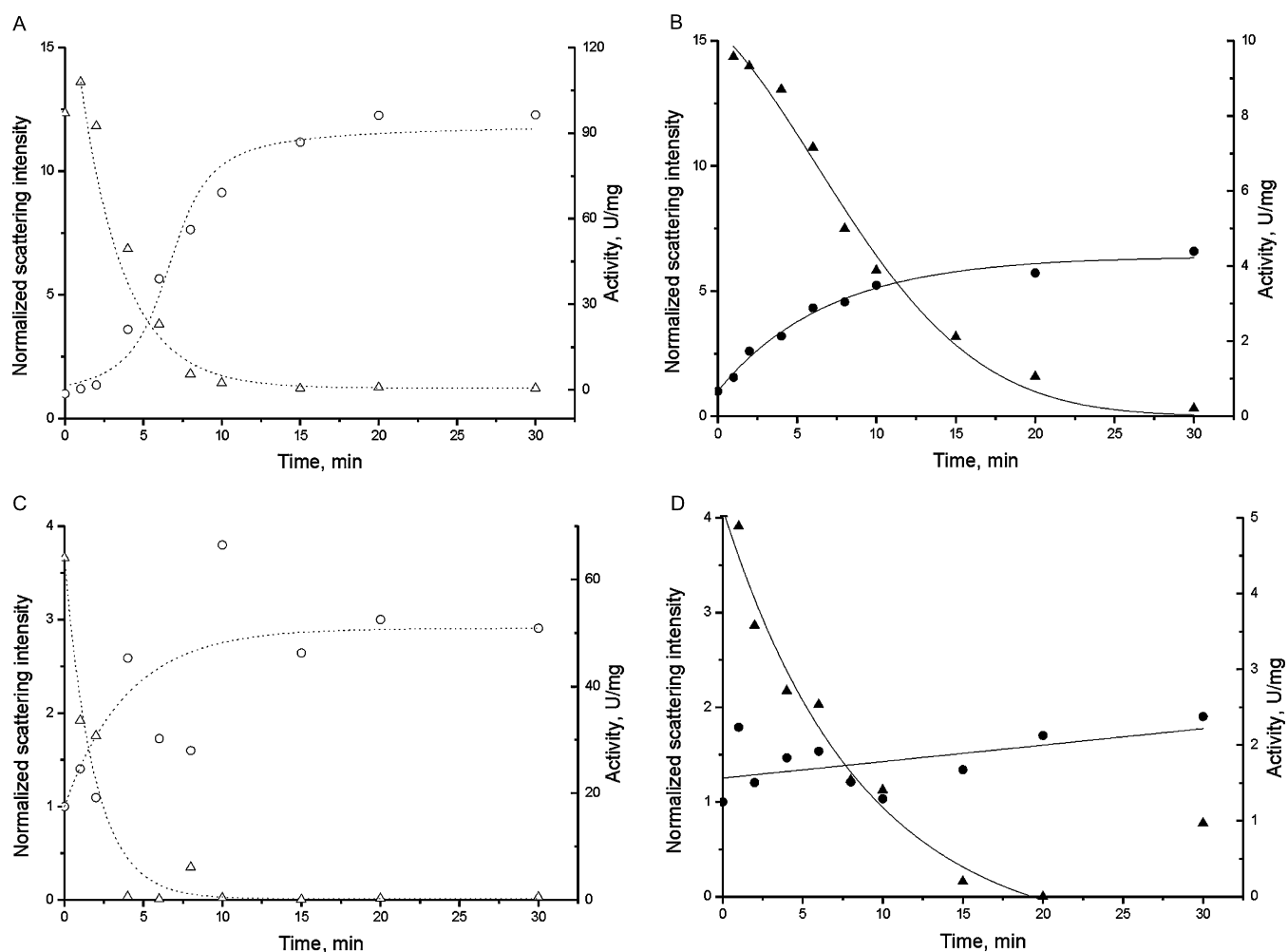


**Fig. 9.** Thermal inactivation and aggregation of *LbADHwt* (white) and *LbADH G37D* (black) followed by static light scattering spectroscopy. The normalized light scattering intensity is depicted in circles, activity data (calculated based on total protein amount) are represented by triangles. A: dissolved *LbADHwt* at 50 °C; B: dissolved *LbADH G37D* at 50 °C; C: solid *LbADHwt* at  $a_w = 0.1$  and  $T = 80$  °C; D: solid *LbADH G37D* at  $a_w = 0.1$  and  $T = 80$  °C. To study the dissolved samples, 0.1 mg/ml solution of the *LbADHwt* or the *LbADH G37D* in 10 mM TEA, 1 mM  $MgCl_2$  buffer at pH 7.5 was divided into 800  $\mu$ l aliquots, heated at 50 °C for 0–30 min and analyzed for light scattering at 450 nm, angle 90° in correlation with the residual enzymatic activity. The solid protein probes were equilibrated over a saturated solution of LiCl for 24 h to reach  $a_w$  of 0.1, then heated at 80 °C for 0–30 min, cooled down to room temperature, re-dissolved in 1 ml of distilled water, and immediately checked for light scattering and enzymatic activity.

reactor, at least for the very similar enzymes studied here. To further prove this hypothesis and to provide an alternative to the solid sample re-dissolution and activity assay, the protein denaturation was followed by spectroscopic measurements to allow a more reliable and direct assay of the protein thermostability.

### 2.6. Investigation of thermal enzyme inactivation by fluorescence spectroscopy

Tryptophan fluorescence spectroscopy was used to follow unfolding of the enzyme variants and to elucidate temperature induced structural changes in the enzymes and relate them to the inactivation process. There are eight tryptophan residues in each of the tetramer *LbADH* molecules, four of them are placed at the surface and thus exposed to the solvent and four are buried between the contacting surfaces of the monomers. The intrinsic tryptophan fluorescence emission spectra of the intact and heat-treated protein samples are shown in Fig. S3 (supplementary material). Conformational changes in the protein structure result in changes of the aromatic amino acids environment, which affects the emission spectra [22]. Comparative studies of the thermal denaturation of both enzyme variants in the solid and dissolved states were

performed using fluorescence spectroscopy paralleled by residual activity measurements. Experiments were designed such that heat-induced inactivation was completed in 30 min. As a control to determine the fluorescence properties related to complete denaturation, urea-induced denaturation of both enzyme variants was monitored by the same method (Fig. 8).

The changes of fluorescence emission maxima and residual activity values of the intact and denatured samples in the presence of increasing urea concentrations (24 h, RT) are shown in Fig. 8A and B. Both enzyme variants show a typical two-state denaturation profile with overlapping inflecting points of the sigmoidal deactivation curves and the emission maxima. From the urea denaturation curves a higher stability in the dissolved state can be deduced for the *LbADH G37D* variant, which reaches the inflection point with 2.5 M urea (24 h, RT), whereas the wild type enzyme's inflection point is reached with 1 M urea (full spectra are provided in Fig. S3, A and B, supplementary information). As was already deduced from residual activity measurements (Fig. 7), *LbADHwt* is generally less thermostable than *LbADH G37D* in aqueous solution. The same was confirmed by additional measurements of the mid-points of thermal transition using CD-spectroscopy (supplementary Fig. S4), which were determined for *LbADHwt* and

the variant *LbADHG37D* to be  $46 \pm 3$  °C and  $59 \pm 6$  °C, respectively. Using fluorescence spectroscopy, we could connect these stability differences to the structural stability. The unfolding in solution at 50 °C, which was detected by fluorescence emission maxima shift analysis, occurred 2-fold faster for the wild type enzyme than for the G37D variant, which coincides with the residual activity measurements (Fig. 8C and D). Using the same experimental approach, it could be shown that the time-course of structural stability loss coincides with residual activity measurements also in the solid samples and does not show significant differences for the wild type enzyme and the G37D variant (Fig. 8E and F). Although both enzymes in the dissolved and solid forms underwent structural changes resulting in a constant shift of emission maxima, the degree of structural unfolding was lower for the solid samples. Despite of the total inactivation, fluorescence emission maxima of the solid samples showed only a red shift of 2.5–5 nm, whereas a red-shift of 8 nm was observed in the liquid samples (Fig. 8C–F). The results are not surprising, as they suggest that less severe structural changes occur in the absence of liquid water. This is corroborated by the measurement of mid-point of thermal inactivation, where no significant decrease in  $\alpha$ -helical content of the solid proteins was observed for temperatures up to 90 °C (data not shown).

The process often following partial unfolding of enzymes is aggregation of the proteins leading to insoluble and inactive enzyme. In order to assess the correlation between deactivation and potential aggregation, which occur in the liquid and dry enzyme samples upon heating, static light scattering was used to investigate the temperature-dependent formation of aggregates in the dissolved enzyme variants incubated at 50 °C and for the solid protein probes, which were heat-inactivated at 80 °C and then re-dissolved in water (Fig. 9). In parallel the residual activity was measured.

These data presented in Fig. 9 show an increase of higher molecular weight species upon incubation at increasing temperatures. For both the liquid and the solid samples these studies clearly demonstrate a correlation between aggregate formation and deactivation. Although aggregate formation is most pronounced in the liquid state it is clearly visible also in the solid samples at least for the wt enzyme.

This effect cannot be observed in Fig. 8 since the residual activity measurements are referred to the soluble protein amount. The different aggregation level of the solid samples of both enzyme variants may be restricted only to temperatures above 70 °C where stronger deviation between half-life of the solid protein was observed (Fig. 7B).

In summary, as could be demonstrated in a reasonable time scale applying higher temperatures (80 °C), heat-induced minor unfolding of the protein structure in the solid state followed by intermolecular aggregation is the suggested process which could cause enzyme inactivation also for gas/solid catalysis. In the reactive system, however, the additional effects due to the presence of the substrates and co-substrates have to be considered, which might increase enzyme inactivation already at lower temperatures.

### 3. Conclusions

In this study, two single-amino-acid exchange enzyme variants, NADPH-dependent *LbADHwt* and NADH-dependent *LbADH G37D* were investigated with respect to their stability both in non-reactive and reactive systems. The aim was to elucidate factors that affect the operational stability in the gas/solid reactor and find parameters that may predict the performance in the gas/solid system.

It could be clearly demonstrated that in spite of a lower thermostability and increased number of degradation products of the cofactor NADPH in comparison to NADH both in the dissolved and

solid state, the cofactor stability does not govern operational stability in the gas/solid reactor system. Measurement of the thermal stabilities of enzymes in solution in the absence of substrates and products is also not indicative for operational stability. However, the thermal stability of the two enzyme variants in the dry state allows the prediction of their stability in the gas/solid system. The latter is of similar order of magnitude for both enzyme variants and corresponds to the base operational stability in the gas/solid reactor at low water activity and low substrate activity.

With increasing thermodynamic activity of water and substrate in the gas/solid reactor differences in the operational stability occur that are probably linked to differences in the catalytic performance of the two enzymes and thus the interaction with the substrate, co-substrate and water molecules. Importantly, at least part of the catalytic differences of the two enzyme variants, *i.e.* the lower affinity to the substrate acetophenone for the variant G37D, can be transferred from observations in the aqueous medium to the gas/solid reactor. Thus, future studies need to further analyze the interaction of substrate and co-substrate with the protein and its effect on the thermostability under non-reactive conditions as well as the effects of variation of the substrate and water activity in the reactive gas/solid reactor system to provide a sound basis for prediction of the operational stability.

At present, the thermostability of the dry enzymes without substrates present has been proven to be predictive for the order of magnitude of the operational stability in the gas/solid reactor and can thus serve for the establishment of screening systems. In future, the identification of further influencing factors would yield the necessary information for an optimization of the gas/solid reactor system for long-term productivity by engineering either the enzyme (microenvironment) or the gas/solid reactor's operating conditions.

## 4. Materials and methods

### 4.1. Chemicals

Media components, salts and substrates for the enzymatic assays were purchased from Sigma–Aldrich. Q-Sepharose and G25 column filling beads were supplied by Pharmacia. High purity  $\beta$ -NADPH and  $\beta$ -NADH were ordered from Biomol GmbH.

### 4.2. Protein over expression and purification

*LbADHwt* and *LbADH G37D* were recombinantly expressed in the pET21a vector purified by ion-exchange chromatography technique as described by Niefind et al. [12]. Purified proteins were desalted on G25 material in 10 mM triethanolamine, 1 mM MgCl<sub>2</sub> buffer (pH 7.5), dissolved to the final concentration of 1 mg/mL, frozen at –20 °C and lyophilized. The dry samples were kept at –20 °C until being used.

### 4.3. Assay of *LbADH* activity

Enzymatic activity of *LbADHwt* and *LbADH G37D* was determined spectrophotometrically by monitoring the decay of NADPH or NADH at 340 nm, respectively [11]. The reaction mixture consisted of 11 mM of acetophenone, 1 mM MgCl<sub>2</sub> and 0.19 mM NAD(P)H in 50 mM TEA buffer, pH 7.0. After pre-heating of the reaction mixture at 30 °C for 5 min, the reaction was started by addition and short mixing of 10  $\mu$ L of the enzyme and was detected by measuring OD<sub>340</sub> against an air blank.

#### 4.4. Protein concentration (Bradford)

Bradford test [23] was applied for the determination of protein concentration in solution. Calibration standards of different dilutions of a BSA stock solution in water as well as the unknown protein concentration was determined by adding 200  $\mu\text{L}$  Bradford reagent to 800  $\mu\text{L}$  of diluted protein solution. Absorbance at 595 nm was measured by means of a UVIKON 922 photometer (Kontron Instruments, UK) after incubation for 5 min. The protein amount in solution could then be determined from the calibration curve.

#### 4.5. Cofactor thermostability studies

The stability of the dissolved cofactors was investigated in a range of 30–70 °C in 50 mM TEA buffer, pH 7.2. *LbADHwt* enzymatic assay was used to measure the residual reducing activity of the heat-treated NADPH samples, *LbADH G37D* was taken for the NADH probes. Solid cofactor probes were directly weighed from supplier's material, were exposed to 50 °C for the time period of 0–24 days, then re-dissolved in 50 mM TEA buffer (pH 7.2) and tested for absorption at 340 nm and reducing activity. Enzymatic assay was performed as described above. The initial highest activity value was taken as 100% and used to normalize the other data.

#### 4.6. HPLC–MS analysis of structure elucidation of cofactor degradation products

Dissolved samples of NADPH and NADH were heated at 50 °C for 16 h in water, whereas the solid cofactor samples were heated at 95 °C for 16 h and subsequently analyzed by HPLC. HPLC–MS experiments were carried out on an Agilent 1100 series binary HPLC system (Agilent Technologies, Waldbronn, Germany), equipped with a DAD (190–400 nm) and coupled with a 4000QTRAP™ linear ion trap mass Spectrometer (Applied Biosystem/MDS SCIEX, Foster City, CA, USA) equipped with a Turbolon spray source.

HPLC separation was achieved on a ZIC–pHILIC PEEK column (SeQuant, Marl, Germany, 150 mm  $\times$  4.6 mm, I.D., 5  $\mu\text{m}$  particle diameter, 200 Å pore size) and a pre-column (20 mm  $\times$  2.1 mm, I.D.) filled with the same material. The isocratic elution was performed with a mixture of acetonitrile and 50 mM ammonium carbonate (pH 8.0) (70:30, v/v) at the flow rate of 0.5 mL/min (split ratio 1:1) kept at 30 °C during analysis. The injection volume was 2  $\mu\text{L}$ . The MS was operated in the positive and negative Enhanced MS (EMS) mode scanning from 100 to 900 Da with a line ion trap (LIT) fill time of 2 ms and a Scan Rate of 4000 Da s<sup>-1</sup>.

The parameters used for all methods were optimized first performing a Flow Injection Analysis (FIA) with NADH as a standard and led to the following parameter settings: IS –4500 V, Declustering Potential (DP) –145 V, Curtain Gas (N<sub>2</sub>) 10 arbitrary units (au), Source Temperature 650 °C, Nebulizer Gas (N<sub>2</sub>) 50 au and Heater Gas (N<sub>2</sub>) 20 au. CE and Q3–Entry barrier were set to –5 V and 8 V, respectively, to minimize fragmentation entering the LIT.

For structure elucidation and confirmation of selected ions highly resolved mass spectra were recorded using a ESI–LTQ–FT Ultra (ThermoFisher Scientific, San Jose, CA, USA), equipped with a 7 T supra-conducting magnet and coupled with the chip-based micro–ESI system NanoMate (Advion BioServices, Ithaca, NY, USA).

The mass spectrometer, used in positive and negative mode, was tuned and external mass calibrated following a standard procedure for all voltages and settings with a calibration solution composed of caffeine, the peptide MRFA and ultramark. Therefore, the settings of the ion optics varied slightly from day to day. The transfer capillary temperature was set to 175 °C.

Hand cut fractions from the analytical HPLC were put in a 96–well plate (zero–carryover) and sprayed continuously by the NanoMate source. The automatic gain control (AGC) was set at

1E4 for ion trap MS scan and 5E5 for FTMS full scan, respectively. Fourier–transform mass spectra were recorded from 100 to 1000 Da at a resolution of 100.000 (at  $m/z$  400), each scan consists from 30 transients.

#### 4.7. Thermostability studies of *LbADH* variants

The dissolved (0.1 mg/mL protein, 10 mM TEA, 1 mM MgCl<sub>2</sub>, pH 7.5) samples of *LbADHwt* and the *LbADH G37D* (each 100  $\mu\text{L}$ ) were incubated in Eppendorf tubes at 30–80 °C in a heating block (Stuart SBH 130D). At specific time points sample tubes were taken and the proteins assayed for residual enzymatic activity as described above. The solid probes were prepared by lyophilization of 100  $\mu\text{L}$  aliquots of the dissolved *LbADHwt* and *LbADH G37D* (0.1 mg/mL protein, 10 mM TEA, 1 mM MgCl<sub>2</sub>, pH 7.5) in Eppendorf tubes. The dry samples were equilibrated with a saturated salt solution of LiCl for 24 h at RT to reach the water activity of 0.1, hermetically closed and incubated at 30–80 °C in a heating block (Stuart SBH 130D). The solid protein probes taken out at specific time points, cooled down on ice for 1 min, re-dissolved in 100  $\mu\text{L}$  of ddH<sub>2</sub>O and analyzed for the residual catalytic activity as described above. The inactivation curves were described by linear, one or second–order exponential decay models. Half–life of enzymatic activity was read from the plots.

#### 4.8. Fluorescence spectroscopy

Thermal denaturation experiments were designed such that heat–induced inactivation was completed in 30 min. Fluorescence emission spectra of the proteins in 10 mM TEA, 1 mM buffer MgCl<sub>2</sub> at pH 7.2 were measured in a LS50B spectrofluorometer (PerkinElmer) in the range 300–450 nm after excitation at 295 nm with a speed of 120 nm min<sup>-1</sup>. Excitation and emission slits were 7.5 nm, respectively. The dissolved samples were measured directly after heat treatment, whereas the solid ones were cooled down and re-dissolved in the corresponding buffer.

The dissolved samples were investigated in the following manner: 0.1 mg/mL solution of *LbADHwt* or *LbADH G37D* in 10 mM TEA, 1 mM MgCl<sub>2</sub> buffer at pH 7.0 was divided into aliquots of 800  $\mu\text{L}$  each, then directly heated at 50 °C for different time intervals and subjected to analysis by fluorescence spectroscopy in correlation with enzymatic activity.

Thermal decomposition of the solid enzyme samples was accomplished as follows: 1 mg/mL solution of *LbADHwt* or *LbADH G37D* in 10 mM TEA, 1 mM MgCl<sub>2</sub> buffer at pH 7.0 were divided into aliquots of 100  $\mu\text{L}$  each as before, then frozen at –20 °C and lyophilized. After lyophilization solid protein probes were heated at 80 °C, cooled down to room temperature, re-dissolved in 1 mL of distilled water, and immediately tested for residual enzymatic activity and fluorescence properties.

#### 4.9. Static light scattering

Static light scattering measurements were performed using a Perkin Elmer LS 50B fluorescence photometer at 450 nm ( $\pm$ 15 nm slit). The scattering curve was obtained at a fixed angle of 90°, in a 400–500 nm range with a 5 nm slit and a scanning rate of 120 nm min<sup>-1</sup>. For a single spectrum, 3 scans were accumulated. The spectra were corrected for the buffer base line. The scattering light intensity was determined at 450 nm. For the easier interpretation of results, the scattering light intensity was normalized to that one of the respective intact enzyme. Experiments with the previously heat incubated *LbADHwt* and *LbADH G37D* were carried out at room temperature. To study the dissolved samples, 0.1 mg/mL solution of the *LbADHwt* or the *LbADH G37D* in 10 mM TEA, 1 mM MgCl<sub>2</sub> buffer at pH 7.5 was divided into 800  $\mu\text{L}$  aliquots, heated

at 50 °C for 0–30 min and analyzed for light scattering at 450 nm, angle 90° in correlation with the residual enzymatic activity. The solid protein probes were equilibrated over a saturated solution of LiCl for 24 h to reach  $a_w$  of 0.1, then heated at 80 °C for 0–30 min, cooled down to room temperature, re-dissolved in 1 mL of distilled water, and immediately checked for light scattering and enzymatic activity.

#### 4.10. Circular dichroism

CD spectra of *LbADHwt* and *LbADH G37D* were recorded using a Jasco J-810 spectro-polarimeter. The measurements were carried out in the range of 190–310 nm, with a scan rate of 50 nm min<sup>-1</sup>. Dissolved proteins were investigated in a quartz cuvette with 1 mm optical pathway, while the solid ones were immobilized by lyophilization on a quartz glass and covered with a second glass. Base line spectra, which were obtained either with buffer or with quartz glasses, were used to correct the data. To determine the midpoint of thermal denaturation ( $T_m$ ) of *LbADHwt* and *LbADH G37D* in the dissolved and the solid state. The protein solution was placed in a quartz cuvette and heated inside the CD photometer cell with a speed of 1 °C min<sup>-1</sup>. Alternatively, enzymes were lyophilized on a quartz glass, covered with another one, placed in the CD polarimeter cell and heated up there. Temperature was varied in a range of 20–80 °C in 5 °C intervals. However, it was impossible to test the residual enzymatic activity and to check the exact temperature values inside the photometer cell. Intact samples of *LbADHwt* or *LbADH G37D* were used as a reference.

#### 4.11. Enzyme immobilization via deposition

Applying a variation of the deposition procedure described in [24], 2.8 mg of lyophilized *LbADHwt* and 12-fold molar excess of NADP<sup>+</sup> relative to the enzyme amount (Biomol GmbH, Hamburg, Germany), were dissolved in 2 mL phosphate buffer ( $I = 50$  mM and pH 7, resulting from KH<sub>2</sub>PO<sub>4</sub> and Na<sub>2</sub>HPO<sub>4</sub> solutions) and mixed together with 1 g glass beads 0.25–0.3 mm (Sartorius AG, Göttingen, Germany) for 30 min in a rotary mixer (RMSW, Welabo, Germany) at 4 °C. Glass beads were washed with distilled water and dried before use. The mixture was dried at 4 °C in a desiccator, containing Silica Gel Orange 2–5 mm (Carl Roth GmbH, Karlsruhe, Germany), with a vacuum pump (CVC 200II, Vacuubrand, Germany) at 300 mbar for 4 h and successively at 40 mbar until dry. For the immobilization of the *LbADH G37D*, 2.8 mg of lyophilized enzyme and a 12-fold molar excess of NADP<sup>+</sup> relative to the amount of enzyme (Biomol GmbH, Hamburg, Germany) were dissolved in 2 mL phosphate buffer and the aforementioned procedure was followed. The enzyme preparations were stored at 4 °C.

#### 4.12. Assay of deposited *LbADH* activity

For measuring the residual activity of the deposited enzyme preparations, both wild type and *LbADH G37D*, the deposited enzyme was previously dissolved from the carriers' surface by means of an appropriate amount of TEA buffer and the activity of the resulting solution was measured as previously described. The activity of the deposited enzyme in IU/mg<sub>carriers</sub> was calculated taking into account the amount of carriers in mg dissolved in the TEA buffer amount in millilitre used.

#### 4.13. Protein loading (Bonde)

In order to determine the amount of protein immobilized on the carriers a Bonde test was carried out [25]. An amount of 10 mg of beads with immobilized enzyme were weighted into a cuvette and 800 μL TEA buffer as well as 200 μL Bradford reagent were added

to the beads and mixed thoroughly. After incubation for 5 min and settling of the beads, the absorbance of the solution was measured at 465 nm by means of a UV-VIS spectrophotometer (UNIKON 922, Kontron Instruments, Italy). The protein amount immobilized on the beads was calculated using a BSA calibration curve.

#### 4.14. Continuous gas/solid enzymatic reactor

A continuous gas/solid enzymatic reactor was constructed according to [26]. The reaction mixture formation and the calculation of the partial pressure of the mixture components (substrates and water) were performed according to [4]. The reactor was operated at 40 °C (reaction temperature) whereas the saturation of the reaction mixture was performed at 45 °C (saturation temperature). The gas mixture had a volumetric flow rate of 20 mL/min. An amount of 50 mg, in the case of the *LbADHwt* and 100 mg in the case of the *LbADH G37D*, of freshly deposited enzyme preparation was dried with nitrogen for 10 min and packed in the reactor between two wool layers, forming a packed bed of 3 mm length. Prior to the reaction onset, the enzyme preparation was thermostated in the reaction unit for approximately 30 min. The progress of the reaction was followed by means of an online gas chromatograph (GC) connected to the outlet of the reactor. The partial pressure of the reactants and products of the reaction mixture were measured by means of the online GC at short intervals, during the reaction progress.

#### 4.15. Online gas chromatography (GC) analysis

The outlet of the reactor was directly connected to an online gas chromatograph (Fisons GC 8000, S+H Analytik, Mönchengladbach, Germany). Sampling was performed via a six-way Valco valve (VICI AG International, Schenkon, Switzerland) maintained at 150 °C. The gas chromatograph was equipped with an FID detector, maintained at 250 °C and a split/split less injector, maintained at 200 °C. The separation was realized through a CP-WAX 52CB (50 m × 0.25 mm × 0.2 μm) GC column (Agilent Technologies, Stuttgart, Germany) at the following temperature program: 2 min at 60 °C, 40 °C/min up to 100 °C, 60 °C/min up to 220 °C and 3 min at 220 °C.

#### 4.16. Data analysis

The conversion  $\xi$  in the reactor at any time point was calculated according to Eq. (1):

$$\xi = \frac{p_{\text{PhEtOH}}}{p_{\text{AcPhO}}} \times 100\% \quad (1)$$

where  $p_{\text{PhEtOH}}$  and  $p_{\text{AcPhO}}$  are the 1-phenylethanol and inlet acetophenone partial pressure, respectively. The initial specific reaction rate  $\nu_0$  [ $\mu\text{mol}/\text{min}/\text{IU}$ ] was calculated according to:

$$\nu_0 = \xi \cdot \frac{Q_{\text{AcPh}}}{100 \times E_0} \quad (2)$$

where  $Q_{\text{AcPh}}$  is the acetophenone molar flow rate in the reactor and  $E_0$  denotes the activity of deposited enzyme packed in the reactor. The activity of the deposited enzyme used for the determination of the specific reaction rate was determined through a residual activity assay before the experiment. The deactivation of the enzyme over time  $t$  was monitored already within the first few hours of reaction. The progress curve was fitted with a 1st order exponential deactivation kinetic, given by Eq. (3) and the initial specific reaction rate  $\nu_0$  as well as deactivation constant  $k_d$  were determined:

$$\nu = \nu_0 \cdot \exp(-k_d \cdot t) \quad (3)$$

The half-life time  $t_{1/2}$  of the enzyme in the gas/solid reactor was calculated through:

$$t_{1/2} = \frac{\ln 2}{k_d} \quad (4)$$

Analysis of exemplary experiments conducted in triplicate indicated that the initial specific reaction rate varied by less than 15% and half-life of the enzyme in the gas/solid reactor by less than 10% from the average.

#### Appendix A. Supplementary data

Supplementary data associated with this article can be found, in the online version, at doi: [10.1016/j.molcatb.2010.09.005](https://doi.org/10.1016/j.molcatb.2010.09.005).

#### References

- [1] S. Lamare, B. Caillaud, K. Roule, I. Goubet, M.D. Legoy, *Biocatalysis and Biotransformation* 19 (2001) 361–377.
- [2] A.H. Trivedi, A.C. Spiess, T. Dausmann, J. Büchs, *Applied Microbiology and Biotechnology* 71 (2006) 407–414.
- [3] F. Parvareh, H. Robert, D. Thomas, M.D. Legoy, *Biotechnology and Bioengineering* 39 (1992) 467–473.
- [4] S. Lamare, M.D. Legoy, M. Graber, *Green Chemistry* 6 (2004) 445–458.
- [5] E. Barzana, M. Karel, A.M. Klivanov, *Biotechnology and Bioengineering* 34 (1989) 1178–1185.
- [6] E. Barzana, A.M. Klivanov, M. Karel, *Applied Biochemistry and Biotechnology* 15 (1987) 25–34.
- [7] C. Ferloni, M. Heinemann, W. Hummel, T. Dausmann, J. Büchs, *Biotechnology Progress* 20 (2004) 975–978.
- [8] F. Yang, A.J. Russel, *Biotechnology and Bioengineering* 49 (1996) 709–716.
- [9] A.H. Trivedi, A.C. Spiess, T. Dausmann, J. Büchs, *Biotechnology Progress* 22 (2006) 454–458.
- [10] M. Müller, M. Wolberg, T. Schubert, W. Hummel, *Advances in Biochemical Engineering/Biotechnology* 92 (2005) 261–287.
- [11] N.H. Schlieben, K. Niefind, J. Müller, B. Riebel, W. Hummel, D. Schomburg, *Journal of Molecular Biology* 349 (2005) 801–813.
- [12] K. Niefind, J. Müller, B. Riebel, W. Hummel, D. Schomburg, *Journal of Molecular Biology* 327 (2003) 317–328.
- [13] H.K. Chenault, G.M. Whitesides, *Applied Biochemistry and Biotechnology* 14 (1987) 147–197.
- [14] A.S. Bommarius, B.R. Riebel, *Biocatalysis—Fundamentals and Applications*, Wiley-CH, 2003.
- [15] W. Liu, P. Wang, *Biotechnology Advances* 25 (2007) 369–384.
- [16] O.H. Lowry, M.K. Rock, D.W. Schulz, J.V. Passonneau, *Journal of Biological Chemistry* 236 (1961) 2746.
- [17] O.H. Lowry, M.K. Rock, J.V. Passonneau, *Journal of Biological Chemistry* 236 (1961) 2756–2759.
- [18] J.T. Wu, L.H. Wu, J.A. Knight, *Clinical Chemistry* 32 (1986) 314–319.
- [19] B.M. Anderson, C.D. Anderson, *The Journal of Biological Chemistry* 238 (1963) 1475–1478.
- [20] K. Dimoula, M. Pohl, J. Büchs, A.C. Spiess, *Biotechnology Journal* 4 (2009) 712–721.
- [21] R. Mikolajek, A.C. Spiess, M. Pohl, S. Lamare, J. Büchs, *Chembiochem* 8 (2007) 1063–1070.
- [22] K. Jack, *Structure in Protein Chemistry*, Garland Publishing, Inc., New York, London, 1995.
- [23] M.M. Bradford, *Analytical Biochemistry* 72 (1976) 248–254.
- [24] A. Trivedi, M. Heinemann, A.C. Spiess, T. Dausmann, J. Büchs, *Journal of Bioscience and Bioengineering* 99 (2005) 340–347.
- [25] M. Bonde, H. Pontoppidan, D.S. Pepper, *Analytical Biochemistry* 200 (1992) 195–198.
- [26] S. Lamare, M.D. Legoy, *Biotechnology Techniques* 9 (1995) 127–132.